Many-Electron Dynamics of a Xe Atom in Strong and Superstrong Laser Fields

K. Yamakawa,* Y. Akahane, Y. Fukuda, M. Aoyama, N. Inoue, H. Ueda, and T. Utsumi

Advanced Photon Research Center, KANSAI Research Establishment, Japan Atomic Energy Research Institute, 8-1 Umemidai, Kizu, Kyoto 619-0215, Japan.

(Received 15 May 2003; revised manuscript received 8 July 2003; published 25 March 2004)

We report on detailed investigations of ionization dynamics of a Xe atom exposed to intense 800-nm pulses of 20-fs duration in the extensive intensity range from 10^{13}–10^{18} W/cm^2. Ion yields of Xe^{+}–Xe^{20+} were observed as a function of laser intensity and compared with the results from a single active electron based Ammosov-Delone-Krainov model. Unexpected ionization probabilities for lower charge states and no interplay between the inner and outer shells by screening are inferred. Suppression of nonsequential ionization towards higher intensity and few optical cycle regimes is also proved.

DOI: 10.1103/PhysRevLett.92.123001 PACS numbers: 32.80.Fb, 32.80.Rm, 42.50.Hz

The presence of strong laser fields radically alters the nature of atomic systems. Understanding the dynamical behavior of atoms exposed to external fields is fundamental toward providing knowledge of properties of matter under such extreme conditions, as well as solutions to control new physical effects for many applications. Over the last two decades a large number of groups have studied the interaction of laser fields with atoms in the regime from multiphoton to tunneling ionization [1]. For instance, highly charged ions up to Xe^{8+} have been produced by using a variety of laser systems with laser intensities of up to $\sim 10^{16}$ W/cm^2 [2–6]. In the tunneling regime, the Ammosov-Delone-Krainov (ADK) model, based on a quasiclassical tunneling theory, provides a relatively good fit to sequential ionization rates of the rare gas atoms [7]. In contrast, simultaneous tunneling of more than one electron (so-called nonsequential ionization) shows experimentally that the production of doubly or multiply charged ions is more effective by many orders of magnitude than predicted by the ADK model [4,8–10]. A number of models and numerical calculations have been applied [8,11–15], but the explanation for this physical mechanism is still not known. Furthermore, most of atomic physics is concerned with the behavior of valence electrons. Therefore, the quest for a many-electron problem of isolated atomic systems remains a distant goal for understanding the behavior of atoms exposed to strong laser fields.

Modern high-power lasers can now access to extraordinary high intensities of 10^{20} W/cm^2 in extremely short durations of 10 fs at unprecedented high repetition rates of 36 000 shots per hour. Such superstrong fields correspond to 60 times the field binding of the ground state electron in the hydrogen atom, and inner shell electrons for heavy (high Z) atoms do not remain within the atomic center. At such intensities the electron velocity in the laser field also becomes relativistic. Thus, the free electrons move at close to the speed of light and their mass changes dramatically compared to their rest mass. Consequentially, it is now possible to test many-electron dynamics of complex atoms in radically new ways. In this Letter, we report on optical field ionization of a Xe atom by 800-nm, 10-Hz laser pulses of 20-fs duration with peak intensities ranging from 10^{13}–10^{18} W/cm^2. The experiments reported herein exhibit three major findings: (i) unexpected ionization probabilities for lower charge states; (ii) no interplay between the inner- and outer-shells by screening; (iii) suppression of nonsequential ionization towards relativistic intensity and also few optical cycle regimes. These new findings have given us a hint of how many-electron systems behave in such fields.

The present work uses a tabletop, next generation Ti:sapphire chirped-pulse amplification (CPA) system [16] that generates 100-TW, 20-fs, 10-Hz pulses with the capability of producing extremely highly charged ions up to Ar^{16+}, Kr^{19+}, and Xe^{26+}, respectively. In order to clarify the ionization dynamics of the Xe atom, measurements of the ion yields as a function of the laser intensity were carried out with the signal-averaging technique at the intensity range from 10^{13}–10^{18} W/cm^2. In our experiment, the linearly polarized laser light was focused using an off-axis parabolic mirror of focal length 161 mm in the center of the ionization chamber having a background pressure below 8×10^{-9} Torr. The Xe pressure in the chamber was controlled typically below 10^{-7} Torr in order to reduce space charge and collective effects. The maximum energy and pulse duration were measured to be 80 mJ and 20 fs, respectively. We obtained the focal spot diameter of 12 μm at $1/e^2$ with 74% of full energy, which corresponds to the estimated maximum intensity of $\sim 6.0 \times 10^{18}$ W/cm^2. The peak to amplifed spontaneous emission intensity contrast ratio was approximately 10^{-6} at a time scale of ± 2 ns. Then, the leading edge of the pulse rises to 10^{-5} at 300 fs and 10^{-2} at 100 fs before the arrival of the pulse peak. We used a half wave plate and polarizer to vary the intensity of the laser pulse. Both of them were placed after the Ti:sapphire amplifier and before the pulse compressor in order to eliminate accumulated B-integral and additional high-order dispersions after compression.

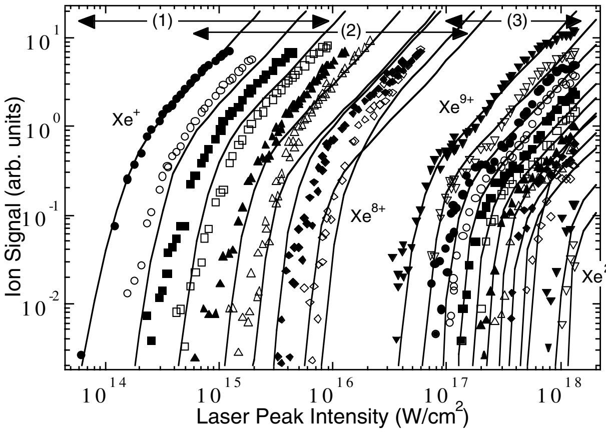

FIG. 1. Comparison of experiment and theory for tunneling ionizations in Xe as a function of laser intensity. Experiment: $\lambda = 800$ nm; $\tau = 20$ fs. Theory: the quasiclassical tunneling theory (solid curves) with no shift in laser intensity. Three sets of intensity scans are indicated: (1) 6×10^{13}–9×10^{15} W/cm^2; (2) 6×10^{14}–1.5×10^{17} W/cm^2; (3) 1×10^{17}–1.5×10^{18} W/cm^2.

Three sets of intensity scans were performed with a combination of different amplifier stages and partial reflection mirrors in the intensity range from (1) 6×10^{13}–9×10^{15} W/cm^2, (2) 6×10^{14}–1.5×10^{17} W/cm^2, and (3) 1×10^{17}–1.5×10^{18} W/cm^2, respectively. The ion species are separated with a 1-m time-of-flight mass spectrometer and detected with dual microchannel plates. An adjustable slit with a width of 300 μm is placed between the acceleration grids and microchannel plate detector on the central axis of the flight tube in order to detect the ions produced in the highest intensity focal region while eliminating the background noise produced by ionizing contaminants in the large focal volume and low-intensity region. A further subtraction of the volume effects was performed by considering integration over a region that is limited by the slit [4]. Each data run consists of 1000 laser shots with the laser energy fluctuations of less than 5%.

The results of the ion-yield data for Xe as a function of laser intensity are shown in Fig. 1. The theoretical curves calculated by the ADK model are also shown as the references in this figure. In this model, only sequential (stepwise) ionization has been considered. It should be noted that all the charge states were produced in the regime of $\gamma < 1$ (Keldysh γ parameter) [17] except for Xe^+ ($\gamma \cong 1$), which indicated we performed the experiment exclusively in the tunneling regime. The results presented in Fig. 1 clearly show disagreement between the experimental ion curves and those from the ADK model along the laser intensity scale. In order to compare between the experimental ion curves and those obtained theoretically, we evaluate a shift factor on each ion curve along the intensity scale by the least-squares method. The shift factor is listed in Table I. The experimental curve of

TABLE I. Shift in theoretical curves needed to match experimental data. The shift factor listed here is the number by which the theoretical intensity scales have been multiplied. For example, a factor of 0.7 means that the theoretical curve for that charge state is shifted lower in intensity by 30%. The values listed under ionization energy are from Ref. [18].

Energy level	Charge state	Ionization energy (eV)	Shift factor
5*p*	1	12.13	1.00
	2	21.21	0.85
	3	32.1	0.70
	4	46.7	0.55
	5	59.7	0.60
	6	71.8	0.75
5*s*	7	92.1	0.90
	8	105.9	0.80
4*d*	9	171	0.95
	10	202	1.00
	11	233	0.90
	12	263	0.85
	13	294	0.80
	14	325	0.85
	15	358	0.80
	16	390	0.80
	17	421	1.00
	18	452	0.90
4*p*	19	549	0.85
	20	583	0.95

Xe^{2+} already begins to disagree with the theoretical one by 15%, while a comparison between the experimental curves of Xe^{3+} to Xe^{6+} and those from the ADK model shows rather poor agreement. For example, the experimental curve of Xe^{4+} disagrees with the theoretical one by nearly 50%. We emphasize that we repeated the measurements several times and saw no discernible shifts in the *relative* positions of all the ion yields data, which means that the disagreements are due to some physical differences in the ionization processes [19]. It should also be pointed out that most of the previous reports focus on finding the knee structure (which is also discussed later on), which is the deviation from the ADK model at the laser intensities below ionization saturation. However, in the cases of $Xe^{3+}$to Xe^{6+}, for example, our experimental data completely disagree with the calculated curves even in the saturation intensity regions.

In general, the atomic ionization energy is a unique and fundamental property for all elements. However, high-precision determinations of the ionization energy, especially for complex atoms, are relatively rare. Even though the factors of 0.5–0.7 for Xe^{3+}–Xe^{6+} completely deviated from the measurement accuracy of the ionization energy mentioned above. Therefore, the influence of the many-electron dynamics in the strong laser field should not be neglected. More surprisingly, the experimental curve for Xe^{9+} returns to fit the theoretical one, subsequently ejecting all the electrons from the $n = 5$ shell of Xe. This result indicates the absence of a relationship between the $4d$ inner shell and the $n = 5$ outer shell. Therefore, we may emphasize that the ionization processes strongly depend on the atomic structure and outermost shell density. So far, a small amount of theoretical work has been carried out to test the dynamics and interplay of outer and inner shells in complex atoms. Boyer and Rhodes [20] and Szöke and Rhodes [21] have suggested that the $4d$ inner shell state of Xe can be strongly excited by coherently driven $5p$ shell electrons. In contrast, L'Huillier *et al.* have shown that the $4d$ inner shell will be shielded from the external field by the outer $5p$ shell [22]. In the latter case, multiple ionization in the $n = 5$ shell, therefore, varies by screening effects. For a given external laser intensity, the effective (local) intensity should increase for each step of the stripping process by screening, increasing the probability for creation of higher charge states. This is what we observe in the experimental ion curves toward lower intensities. Considering the result in the case of Xe^{9+}, it is also favorable to the case suggested by L'Huillier *et al.* It is simply explained as follows. Stripping of the outer shell occurs by the leading edge of the pulse, which reduces the screening. The effective intensity in the $4d$ inner shell then approaches the given external intensity and leads to sequential tunneling ionization. As for the charge state of Xe^{19+}, the experimental curve differs from the theoretical one by 15%. Although the transition from the $4d$ to $4p$ subshells (ionization potentials from 452 to 549 eV) [18] is relatively large, it might be possible for the existence of some coupling mechanisms among these electrons in those subshells as they are more tightly bound. There should be a limit to apply their analysis in our experimental regime since it is based only on the framework of the perturbation theory. However, it is difficult to make a general statement at the moment, because it will probably take quite some time for the theory to provide reasonably systematic description of the role of implications of many electrons in strong and superstrong laser fields. Our observation should aid in distinguishing between the viability of future models.

As part of the comparison between the experimental curves and those obtained theoretically, we shift the theoretical curves along the laser intensity scale to match the data in order to look at the presence of the knee structures described previously. This is presented in Fig. 2 and made based on the shift factor listed in Table I. From Fig. 2, it is clear that the experimental ion yields of Xe^{2+}–Xe^{7+} are more effective by orders of magnitude than predicted by the ADK model at the laser intensities below saturation of ionizations while the ion yields of Xe^{8+}–Xe^{20+} can be thought to follow the calculations. The discrepancies in Xe^{2+}–Xe^{7+} yield between the experiment and the ADK model at these intensities are a signature of nonsequential (NS) ionization. To compare our result with the previous ones by other groups, we refer the experiment for sixfold ionizations of Xe with a femtosecond Ti:sapphire laser pulse [4]. The experimental data presented in Ref. [4] have also been compared with the results [23] of the correlated energy sharing model, based on the so-called "intense-field many-body S-matrix theory" (IMST) [14]. The calculated results for the ion yields of the charge states up to Xe^{6+} were found to agree remarkably well with the measured ones. Considering the situation of our results, we first found that the total probabilities of NS ionization for Xe^{2+}–Xe^{7} were much lower than seen in Ref. [23]. The rescattering model [11] explains NS ionization by the possibility of an inelastic collision between the returned electron driven by the oscillating laser field and its parent ion, which can result in further ionization of the second electron. In this manner the NS ionization yield depends on the number of returns of the electron and, therefore, on the number of optical cycles of the laser pulse [24]. Indeed, the experiment described in Ref. [4] was performed with a 200-fs duration ($\sim$ 80 optical cycles), 800-nm pulse, whereas the experiment described here used a 20-fs duration ($\sim$ 8 optical cycles), 800-nm pulse.

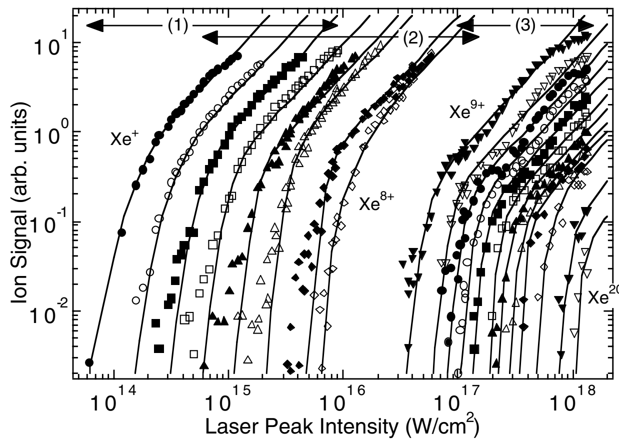

FIG. 2. Comparison of experiment and theory for tunneling ionizations in Xe as a function of laser intensity that is identical to Fig. 1, but with shift of the theoretical curves along the laser intensity scale to match the experimental data. The solid curves (theory) represent the "best fit" to the data based on the shift factor listed in Table I.

Although the IMST calculation of the ion yields for the charge states higher than Xe^{8+} has not yet been performed, from a classical point of view, the tendency of the ionic charge state yields of over Xe^{9+} can be qualitatively explained by suppression of NS ionization with increasing laser intensities towards the relativistic regime [25]. In this regime the magnetic field component is no longer negligible, causing a forward drift momentum of photoelectrons in the laser propagation direction. It means that the Lorentz force in this superstrong field may reduce rescattering of laser-driven electrons. For example, a result of a classical trajectory of the ionized electron by our one-dimensional calculation shows that the displacement of the electron along the laser propagation direction is of the order of 10 nm over the half laser cycle at the laser intensity of 10^{17} W/cm^2. Then, the electron loses the parent ion and no rescattering will occur. Our experimental result, therefore, confirms the indirect evidence for the suppression of NS ionization of Xe at the *fixed* relativistic laser intensity [26]. As for the charge state of Xe^{8+} at the laser intensity of around 10^{16} W/cm^2, however, the magnetic field component at this intensity seems to be not strong enough to induce the displacement of the returning electrons (on the order of a few angstroms over the half laser cycle). Consequently, the suppression of NS ionization for Xe^{8+}, and certainly higher ones, is also probably due to the small core size with the decrease in the inelastic scattering cross section, as well as the reduction of the laser optical cycles mentioned previously.

In summary, we have studied the interaction of strong laser fields with the Xe atom, spanning the peak intensity range from 10^{13} to 10^{18} W/cm^2. It is concluded that the conventional treatments of multiple ionization do not correspond to our experimental findings for the many-electron atom. The essential findings were (i) unexpected ionization probabilities for lower charge states, (ii) no interplay between the inner and outer shells by screening, and (iii) suppression of nonsequential ionization towards relativistic intensity and few optical cycle regimes. These new findings have given us a hint of how many-electron systems behave in such fields. At last, a quantitative theory of relativistic ionization of hydrogenlike ions is being approached recently [27]. Therefore, an understanding of the many-electron problem in isolated atomic systems remains a distant goal.

The authors acknowledge C. H. Keitel and F. H. M. Faisal for fruitful discussions in the early stage of this work. They also thank T. Kimura, T. Tajima, and Y. Kato for their encouragement. This research was partly supported by a Grant-in-Aid for Specially Promoted Research (Contract No. 15002013) of the Ministry of Education, Culture, Sports, Science and Technology of Japan.

*Electronic address: yamakawa@apr.jaeri.go.jp

[1] For recent review, see, e.g., *Multiphoton Processes*, edited by L. F. DiMauro, R. R. Freeman, and K. C. Kulander, AIP Conf. Proc. No. 525 (AIP, New York, 2000).
[2] S. L. Chin, W. Xiong, and P. Lavigne, J. Opt. Soc. Am. B **4**, 853 (1987).
[3] S. Augst *et al.*, Phys. Rev. Lett. **63**, 2212 (1989).
[4] S. Larochelle, A. Talebpour, and S. L. Chin, J. Phys. B **73**, 1201 (1998).
[5] M. D. Perry *et al.*, Phys. Rev. Lett. **60**, 1270 (1988).
[6] T. S. Luk *et al.*, Phys. Rev. Lett. **51**, 110 (1983).
[7] M. V. Ammosov, N. B. Delone, and V. P. Krainov, Zh. Eksp. Teor. Fiz. **9**, 2008 (1986) [Sov. Phys. JETP **64**, 1191 (1986)].
[8] D. N. Fittinghoff *et al.*, Phys. Rev. Lett. **69**, 2642 (1992).
[9] B. Walker *et al.*, Phys. Rev. Lett. **73**, 1227 (1994).
[10] Th. Weber *et al.*, Nature (London) **405**, 658 (2000).
[11] P. B. Corkum, Phys. Rev. Lett. **73**, 1994 (1993).
[12] J. B. Watson *et al.*, Phys. Rev. Lett. **78**, 1884 (1997).
[13] K. T. Taylor *et al.*, Laser Phys. **9**, 98 (1999).
[14] A. Becker and F. H. M. Faisal, Phys. Rev. A **59**, R1742 (1999).
[15] U. Eichmann *et al.*, Phys. Rev. Lett. **84**, 3550 (2000).
[16] K. Yamakawa *et al.*, Opt. Lett. **23**, 1468 (1998).
[17] L. V. Keldysh, Zh. Eksp. Teor. Fiz. **47**, 1945 (1964) [Sov. Phys. JETP **20**, 1307 (1965).
[18] R. D. Cowan, *The Theory of Atomic Structure and Spectra* (The University of California Press, Berkely, 1981).
[19] We have also obtained good agreement between the experimental ion curves and those from the ADK model for lower charge states of Ar and Kr with no shift in laser intensity scale.
[20] K. Boyer and C. K. Rhodes, Phys. Rev. Lett. **54**, 1490 (1985).
[21] A. Szöke and C. K. Rhodes, Phys. Rev. Lett. **56**, 720 (1986).
[22] A. L'Huillier, L. Jönsson, and G. Wendin, Phys. Rev. A **33**, 3938 (1986).
[23] A. Becker and F. H. M. Faisal, Phys. Rev. A **59**, R3182 (1999).
[24] V. R. Bhardwaj *et al.*, Phys. Rev. Lett. **86**, 3522 (2001).
[25] C. H. Keitel and P. L. Knight, Phys. Rev. A **51**, 1420 (1995).
[26] M. Dammasch *et al.*, Phys. Rev. A **64**, 061402R (2001).
[27] N. Milosevic, V. P. Krainov, and T. Brabec, Phys. Rev. Lett. **89**, 193001 (2002).